

Supplementary Material to: Robust Incremental SLAM under Constrained Optimization Formulation

Fang Bai, Teresa Vidal Calleja, and Shoudong Huang

Abstract—This is the supplementary material to the paper entitled “Robust Incremental SLAM under Constrained Optimization Formulation”. Accepted by IEEE Robotics and Automation Letters (RA-L), with ICRA conference option on January 3, 2018.

I. PRELIMINARIES ON $SO(3)$ GROUP

A. A Brief Introduction to $SO(3)$ Group

The definition of special orthogonal group ($SO(3)$ group) is the set of valid rotation matrices

$$SO(3) \stackrel{\text{def}}{=} \{\mathbf{R} \in \mathbb{R}^{3 \times 3} | \mathbf{R}\mathbf{R}^T = \mathbf{I}, \det(\mathbf{R}) = 1\}.$$

The Lie algebra of $SO(3)$ (denoted by $\mathfrak{so}(3)$), is usually referred as a set of skew-symmetric matrices which can be identified by an element in \mathbb{R}^3 . Denote the skew-symmetric matrix associated with $\Theta \in \mathbb{R}^3$ as $[\Theta]_{\times} \in \mathfrak{so}(3)$, then

$$[\Theta]_{\times} = \begin{bmatrix} 0 & -\theta_3 & \theta_2 \\ \theta_3 & 0 & -\theta_1 \\ -\theta_2 & \theta_1 & 0 \end{bmatrix} \in \mathfrak{so}(3).$$

For each rotation \mathbf{R} , there is an axis-angle representation Θ . The rotation matrix \mathbf{R} and its corresponding axis-angle Θ are connected by exponential mapping $\text{Exp}(\cdot)$ and logarithm mapping $\text{Log}(\cdot)$ as below.

$$SO(3) \ni \mathbf{R} = \text{Exp}(\Theta) = \mathbf{I} + \frac{[\Theta]_{\times}}{\|\Theta\|} \sin \|\Theta\| + \frac{[\Theta]_{\times}^2}{\|\Theta\|^2} (1 - \cos \|\Theta\|)$$

$$\mathbb{R}^3 \ni \Theta = \text{Log}(\mathbf{R}) = \frac{\theta}{2 \sin \theta} \begin{bmatrix} r_{32} - r_{23} \\ r_{13} - r_{31} \\ r_{21} - r_{12} \end{bmatrix}$$

where $\theta = \cos^{-1}(\frac{\text{trace}(\mathbf{R})-1}{2})$, $r_{ij} \in \mathbb{R}$ is the ij -th elements of the rotation matrix \mathbf{R} .

The BCH formula to incorporate the perturbation on $SO(3)$ into the axis-angle space is presented as,

$$\text{Exp}(\Theta_1) \cdot \text{Exp}(\Theta_2) \approx \begin{cases} \text{Exp}[\mathbf{J}_r^{-1}(-\Theta_2) \cdot \Theta_1 + \Theta_2] & \Theta_1 \rightarrow \mathbf{0} \\ \text{Exp}[\Theta_1 + \mathbf{J}_r^{-1}(\Theta_1) \cdot \Theta_2] & \Theta_2 \rightarrow \mathbf{0} \end{cases}$$

where $\mathbf{J}_r(\cdot)$ is the so-called right-hand Jacobian given by

$$\mathbf{J}_r(\Theta) = \mathbf{I} - \frac{1 - \cos \|\Theta\|}{\|\Theta\|^2} [\Theta]_{\times} + \frac{\|\Theta\| - \sin \|\Theta\|}{\|\Theta\|^3} [\Theta]_{\times}^2.$$

If $\Theta = \mathbf{0}$, $\mathbf{J}_r(\Theta) = \mathbf{I}$.

An identity as below derived from the adjoint operation of $SO(3)$ is

$$\mathbf{R} \cdot \text{Exp}(\Theta) \cdot \mathbf{R}^T = \text{Exp}(\mathbf{R}\Theta).$$

The authors are with the Centre for Autonomous Systems (CAS), University of Technology Sydney, Australia. Email: Fang.Bai@student.uts.edu.au, {Teresa.VidalCalleja, Shoudong.Huang}@uts.edu.au.

B. Properties

Some properties for $SO(3)$ group are listed as below.

$$[\Theta_1]_{\times} \cdot \Theta_2 = -[\Theta_2]_{\times} \cdot \Theta_1, \quad \forall \Theta_1, \Theta_2 \in \mathbb{R}^3$$

$$\mathbf{R} \cdot [\Theta]_{\times} \cdot \mathbf{R}^T = [\mathbf{R}\Theta]_{\times}, \quad \forall \Theta \in \mathbb{R}^3, \mathbf{R} \in SO(3)$$

$$\text{Exp}(\Theta) \approx \mathbf{I} + [\Theta]_{\times} + \frac{1}{2}[\Theta]_{\times}^2, \quad \text{if } \mathbb{R}^3 \ni \Theta \rightarrow 0$$

$$\mathbf{R} \cdot \text{Exp}(\Theta) = \text{Exp}(\mathbf{R}\Theta) \cdot \mathbf{R}, \quad \forall \Theta \in \mathbb{R}^3, \mathbf{R} \in SO(3)$$

II. LINEARIZATION OF THE CONSTRAINED SLAM FORMULATION

A. Linearization of the Translational Equation

The linearization of the translational equation can be attained by firstly linearizing terms like

$$\mathbf{F}_c = [\prod_{i=1}^m \mathbf{R}_i] \mathbf{y} \quad (\mathbf{R}_i \in SO(3), \mathbf{y} \in \mathbb{R}^3)$$

then collecting the linearized terms together to obtain a full linearized version.

Let $\Omega_m^n = \prod_{i=m}^n \mathbf{R}_i$, then \mathbf{F}_c can be written as

$$\mathbf{F}_c = [\prod_{i=1}^m \mathbf{R}_i] \mathbf{y} = \Omega_1^{j-1} \cdot \mathbf{R}_j \cdot \Omega_{j+1}^m \mathbf{y}.$$

For \mathbf{R}_j and \mathbf{y} , add a perturbation on their current estimate $\check{\mathbf{R}}_j$ and $\check{\mathbf{y}}$ respectively, then approximate the rotational perturbation with its second-order approximation, which results

$$\mathbf{R}_j = \check{\mathbf{R}}_j \cdot \text{Exp}(\Theta_j) \approx \check{\mathbf{R}}_j \cdot (\mathbf{I} + [\Theta_j]_{\times} + \frac{1}{2}[\Theta_j]_{\times}^2)$$

$$\mathbf{y} = \check{\mathbf{y}} + \mathbf{y}_m$$

where $\Theta_j \rightarrow \mathbf{0}$, $\mathbf{y}_m \rightarrow \mathbf{0}$.

By Taylor expansion, at point $\mathbf{y}_m = \mathbf{0}$, $\Theta_j = \mathbf{0}$ ($j = 1, \dots, m$), we have

$$\mathbf{F}_c = \mathbf{F}_c|_0 + \frac{\partial \mathbf{F}_c}{\partial \mathbf{y}_m}|_0 \mathbf{y}_m + \sum_{j=1}^m \frac{\partial \mathbf{F}_c}{\partial \Theta_j}|_0 \Theta_j + \mathbf{o}$$

$$\begin{aligned} \frac{\partial \mathbf{F}_c}{\partial \Theta_j}|_0 &= \frac{\partial}{\partial \Theta_j} \{ \Omega_1^{j-1} \cdot \check{\mathbf{R}}_j \cdot (\mathbf{I} + [\Theta_j]_{\times} + \frac{1}{2}[\Theta_j]_{\times}^2) \cdot \Omega_{j+1}^m \mathbf{y} \}|_0 \\ &= \frac{\partial}{\partial \Theta_j} \{ \Omega_1^{j-1} \cdot \check{\mathbf{R}}_j \cdot [\Theta_j]_{\times} \cdot \Omega_{j+1}^m \mathbf{y} \}|_0 \\ &= \frac{\partial}{\partial \Theta_j} \{ -\Omega_1^{j-1} \cdot \check{\mathbf{R}}_j \cdot [\Omega_{j+1}^m \mathbf{y}]_{\times} \cdot \Theta_j \}|_0 \\ &= -\Omega_1^{j-1} \cdot \check{\mathbf{R}}_j \cdot [\Omega_{j+1}^m \mathbf{y}]_{\times}|_0 \\ &= -\check{\Omega}_1^{j-1} \cdot \check{\mathbf{R}}_j \cdot [\check{\Omega}_{j+1}^m \check{\mathbf{y}}]_{\times} \\ &= -\check{\Omega}_1^j [\check{\Omega}_{j+1}^m \check{\mathbf{y}}]_{\times} \end{aligned}$$

$$\left. \frac{\partial \mathbf{F}_c}{\partial \mathbf{y}_m} \right|_0 = \frac{\partial}{\partial \mathbf{y}_m} \left\{ \left[\prod_{i=1}^m \mathbf{R}_i \right] (\check{\mathbf{y}} + \mathbf{y}_m) \right\} \Big|_0 = \left[\prod_{i=1}^m \mathbf{R}_i \right] \Big|_0 = \left[\prod_{i=1}^m \check{\mathbf{R}}_i \right] = \check{\mathbf{\Omega}}_1^m$$

$$\mathbf{F}_c \Big|_0 = \left[\prod_{i=1}^m \mathbf{R}_i \right] \mathbf{y} \Big|_0 = \left[\prod_{i=1}^m \check{\mathbf{R}}_i \right] \check{\mathbf{y}} = \check{\mathbf{\Omega}}_1^m \check{\mathbf{y}}$$

Note here we use notation $\check{\mathbf{\Omega}}_m^n = \prod_{i=m}^n \check{\mathbf{R}}_i$.

Thus, after linearization

$$\mathbf{F}_c = \check{\mathbf{\Omega}}_1^m \check{\mathbf{y}} + \check{\mathbf{\Omega}}_1^m \mathbf{y}_m - \sum_{j=1}^m \check{\mathbf{\Omega}}_1^j [\check{\mathbf{\Omega}}_{j+1}^m \check{\mathbf{y}}] \times \Theta_j + \mathbf{o}.$$

B. Linearization of the Rotational Equation

For the rotational equation, a term in the form like

$$\prod_{i=1}^m \mathbf{R}_i = \mathbf{R}_1 \mathbf{R}_2 \cdots \mathbf{R}_m = \mathbf{R}_0$$

needs to be linearized.

For each rotation \mathbf{R}_i ($i = 0, 1, \dots, m$), adding a perturbation Θ_i in the axis-angle space at its current estimate $\check{\mathbf{R}}_i$, the constraint can be written as

$$\prod_{i=1}^m [\check{\mathbf{R}}_i \mathbf{Exp}(\Theta_i)] = \check{\mathbf{R}}_0 \mathbf{Exp}(\Theta_0). \quad (1)$$

Using the identity

$$\mathbf{R} \cdot \mathbf{Exp}(\Theta) = \mathbf{Exp}(\mathbf{R}\Theta) \cdot \mathbf{R}$$

iteratively, the left-hand side of (1) becomes

$$\begin{aligned} \prod_{i=1}^m [\check{\mathbf{R}}_i \mathbf{Exp}(\Theta_i)] &= \left\{ \prod_{i=1}^m \mathbf{Exp} \left(\left[\prod_{j=1}^i \check{\mathbf{R}}_j \right] \cdot \Theta_i \right) \right\} \cdot \prod_{i=1}^m \check{\mathbf{R}}_i \\ &\approx \mathbf{Exp} \left(\sum_{i=1}^m \left[\prod_{j=1}^i \check{\mathbf{R}}_j \right] \cdot \Theta_i \right) \cdot \prod_{i=1}^m \check{\mathbf{R}}_i. \end{aligned}$$

Hence (1) takes the form

$$\mathbf{Exp} \left(\sum_{i=1}^m \left[\prod_{j=1}^i \check{\mathbf{R}}_j \right] \cdot \Theta_i \right) \cdot \prod_{i=1}^m \check{\mathbf{R}}_i \approx \mathbf{Exp}(\check{\mathbf{R}}_0 \Theta_0) \cdot \check{\mathbf{R}}_0.$$

Let $\eta = \mathbf{Log}(\check{\mathbf{R}}_0 \cdot [\prod_{i=1}^m \check{\mathbf{R}}_i]^\top)$, then

$$\mathbf{Exp}(-\check{\mathbf{R}}_0 \Theta_0 + \sum_{i=1}^m \left[\prod_{j=1}^i \check{\mathbf{R}}_j \right] \cdot \Theta_i) \cdot \mathbf{Exp}(-\eta) \approx \mathbf{I}.$$

Using BCH formula, it can be written as

$$\mathbf{Exp}(\mathbf{J}_r^{-1}(\eta) \{-\check{\mathbf{R}}_0 \Theta_0 + \sum_{i=1}^m \left[\prod_{j=1}^i \check{\mathbf{R}}_j \right] \cdot \Theta_i\} - \eta) \approx \mathbf{I}.$$

The axis-angle space takes the form

$$\mathbf{J}_r^{-1}(\eta) \{-\check{\mathbf{R}}_0 \Theta_0 + \sum_{i=1}^m \left[\prod_{j=1}^i \check{\mathbf{R}}_j \right] \cdot \Theta_i\} - \eta \approx \mathbf{0} \quad (2)$$

if Θ_i and η are small.

Equivalently, (2) can be written as

$$-\check{\mathbf{R}}_0 \Theta_0 + \sum_{i=1}^m \left[\prod_{j=1}^i \check{\mathbf{R}}_j \right] \cdot \Theta_i \approx \mathbf{J}_r(\eta) \eta.$$

C. Linearization of the Objective Function

The only non-linear part of the objective lies in the logarithm mapping which can be linearized as follow.

$$\begin{aligned} \mathbf{Log}(\mathbf{Z}_{R_j^i}^\top \mathbf{R}_j^i) &= \mathbf{Log}\{\mathbf{Z}_{R_j^i}^\top \check{\mathbf{R}}_j^i \cdot \mathbf{Exp}(\Theta_j^i)\} \\ &= \mathbf{Log}\{\mathbf{Exp}(\eta_{R_j^i}) \cdot \mathbf{Exp}(\Theta_j^i)\} \\ &\approx \mathbf{Log}\{\mathbf{Exp}[\eta_{R_j^i} + \mathbf{J}_r^{-1}(\eta_{R_j^i}) \Theta_j^i]\} \\ &= \eta_{R_j^i} + \mathbf{J}_r^{-1}(\eta_{R_j^i}) \Theta_j^i \end{aligned}$$

where $\eta_{R_j^i} = \mathbf{Log}(\mathbf{Z}_{R_j^i}^\top \check{\mathbf{R}}_j^i)$.

III. INDEPENDENT CONSTRAINTS/LOOP-CLOSURES

Continued from Section VI.B.

The independence of the loop-closure cycles in each subgraph can be further assessed as follow:

Each loop-closure cycle in the subgraph can be uniquely described by three nodes: the common end-node, the first and last node connecting the end-node in the loop-closure cycle. For instance in Fig. 2d in the paper, there are six loop-closure cycles, which can be described by the nodes sequence 5-1-2, 5-1-3, 5-1-4, 5-2-3, 5-2-4, 5-3-4. Since the end-node 5 is the same, the loop-closure cycles can be further represented by six pairs (1,2), (1,3), (1,4), (2,3), (2,4), (3,4). From which, we take some pairs as edges of an undirected graph g . The constraints/loop-closure cycles are independent if the corresponding pairs do not constitute cycles in g .

For example, in Fig. 1, the edge pairs in the first row (these graphs are non-cyclic) indicate independent loop-closures, while the edge pairs in the second row (these graphs are cyclic) indicate non-independent loop-closures. The simple fact can be easily verified by taking edge pairs, for instance, in Fig. 1c, (1,2), (1,3), (2,4), along with node 5, which constitute loop-closures 5-1-2, 5-1-3, 5-2-4, these loop-closures are independent since Fig. 1c contains no cycles. On the contrary, in Fig. 1g, edge pairs (1,2), (1,3), (2,4), (3,4) along with node 5, constitute a set of non-independent loop-closures 5-1-2, 5-1-3, 5-2-4, 5-3-4, because of there is a cycle in Fig. 1g.

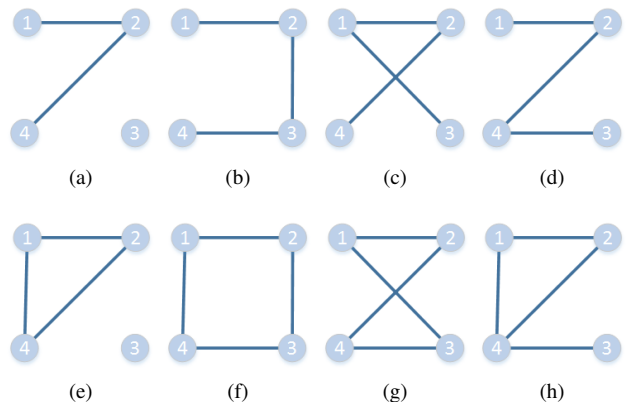


Fig. 1. The relationship of independence and cycles.

IV. ADDITIONAL RESULTS

A. MITb

The initial odometry of MITb is shown in Fig. 2a. In the outlier free case, a simple Gauss-Newton will converge to a local minimum (Fig. 2b), while the global minimum can be readily recovered by iSQP, DCS, or Cauchy (refined with Gauss-Newton) as shown in Fig. 2c.

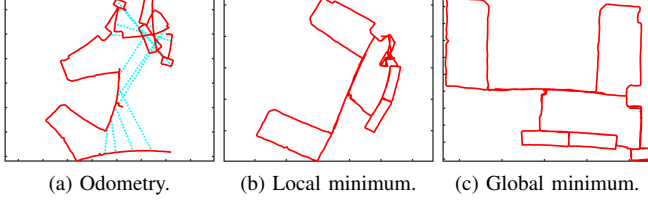


Fig. 2. The odometry, local minimum and global minimum of the MITb dataset.

B. Manhattan and Intel dataset

Actually, for dataset like Manhattan and Intel with dense loop-closures, applying the constraint metric in Section VI.A is not computationally efficient since matrix \mathbf{AQA}^\top can become dense. However, in this case, it is not necessary to stick to the metric in Section VI.A, since the noise level of the dataset is small and a heuristic approach can also work well in practice. Below are examples using Euclidean norm as the constraint metric to select constraints in presence of 500 outliers for the Intel dataset (Fig. 3) and the Manhattan dataset (Fig. 4).

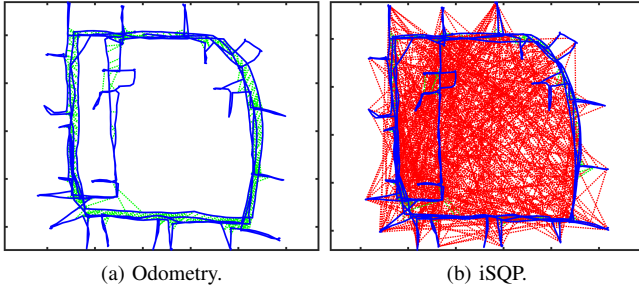


Fig. 3. Intel dataset with 500 outliers.

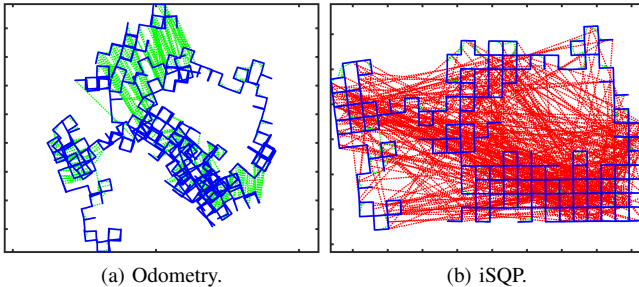


Fig. 4. Manhattan dataset with 500 outliers.

Mathematically, at solution \mathbf{x}_{k-1} , we use $\frac{1}{\log N} \|\mathbf{C}_i(\mathbf{x}_{k-1})\|_2$ to select constraints, where N is the number of edges involved in the loop-closures cycle (indicating the size of the loop-closure cycle). A threshold based on the ratio in terms of the current constraint metric over the median of the

history constraint metrics are used to replace χ^2 difference test.

Note that this simple Euclidean norm based metric prefers small loop-closure cycles to big loop-closure cycles, because less error is accumulated in small loop-closure cycles. This induces ambiguity in face of big correct loop-closures (inliers) and small incorrect loop-closures (outliers). Thus this heuristic approach does not work well for the dataset with sparse loop-closures like MITb (actually fails catastrophically with only 2 outliers). However, with sufficient number of candidate loop-closures, the error in big correct loop-closures can be reduced by the previous added small correct loop-closures. Thus the Euclidean norm based metric can work in datasets with low noise levels and dense loop-closures.

C. Sphere400

The Sphere400 dataset is simulated using the command “create_sphere” in g2o, with 400 poses and 1120 loop-closure edges. The initial odometry is shown in Fig. 5a. We add 500 outliers and solve the dataset with iSQP. The result is shown in Fig. 5b. We use a mixed strategy of the Euclidean

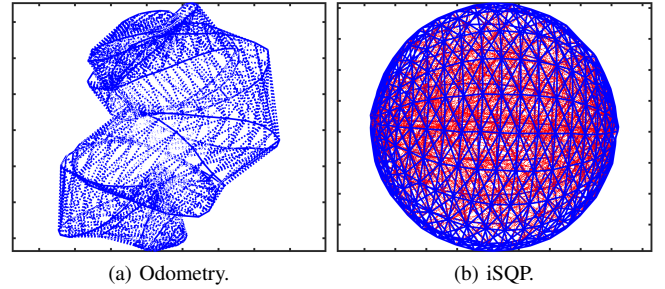


Fig. 5. Sphere400 dataset with 500 outliers.

norm based metric $\frac{1}{\log N} \|\mathbf{C}_i(\mathbf{x}_{k-1})\|_2$ and the probabilistic constraint metric in Section VI.A, where we use Euclidean norm based metric for constraints that yield small Euclidean residual errors $\|\mathbf{C}_i(\mathbf{x}_{k-1})\|_2$, and the probabilistic metric for constraints that yield large Euclidean residual errors.

V. DISCUSSION

As mentioned in the paper, it is also possible to choose $SE(3)$ optimization techniques by considering the translational and rotational part together as $SE(3)$ transformations. The linearization on $SE(3)$ is very similar to the linearization of the rotational equation described in Section II-B. However, to generalize the implementation of pose-graph SLAM and feature-based SLAM, we stick to $SO(3)$ linearization techniques here.

It is worth mentioning that the covariance for $SE(3)$ and $SO(3)$ are slightly different. For the rotational part, the covariance are exactly the same. However for the translational part, the covariance for $SO(3)$ and $SE(3)$ are related by

$$\mathbf{R}_z \cdot \Sigma_T \cdot \mathbf{R}_z^\top = \Omega_T$$

Here \mathbf{R}_z is the rotational part of the relative pose measurement data, and Σ_T is the covariance for the translational part

in $SE(3)$ while Ω_T is that in $SO(3)$. This can be examined easily by considering the translational and rotational part in $SE(3)$ separately.